



HAL
open science

Reception tests of the WEST PFUs using ultrasonic testing and infrared thermography

M. Ramaniraka, M. Richou, N. Vignal, Y. Addab, M. Missirlian

► **To cite this version:**

M. Ramaniraka, M. Richou, N. Vignal, Y. Addab, M. Missirlian. Reception tests of the WEST PFUs using ultrasonic testing and infrared thermography. Nuclear Materials and Energy, 2022, 32, pp.101210. 10.1016/j.nme.2022.101210 . hal-03887799

HAL Id: hal-03887799

<https://hal.science/hal-03887799v1>

Submitted on 22 Jul 2024

HAL is a multi-disciplinary open access archive for the deposit and dissemination of scientific research documents, whether they are published or not. The documents may come from teaching and research institutions in France or abroad, or from public or private research centers.

L'archive ouverte pluridisciplinaire **HAL**, est destinée au dépôt et à la diffusion de documents scientifiques de niveau recherche, publiés ou non, émanant des établissements d'enseignement et de recherche français ou étrangers, des laboratoires publics ou privés.



Distributed under a Creative Commons Attribution - NonCommercial 4.0 International License

Reception tests of the WEST PFUs using ultrasonic testing and infrared thermography

M. Ramaniraka¹, M. Richou¹, N. Vignal¹, Y. Addab¹, M. Missirlian¹

¹CEA, IRFM, F-13108 Saint-Paul-lez-Durance, France

Abstract

This study compiles the results of the acceptance and reception tests of the 456 WEST plasma facing units (PFUs) using ultrasonic testing, infrared (IR) thermography and high heat flux (HHF) tests. The actively cooled PFU, based on manufacturing technologies options foreseen for the ITER divertor target, is constituted of 35 tungsten blocks joint to CuCrZr tube via Cu-OFHC interlayer. The typical defect leading to an adequate heat exhaust of the component is the debonding at blocks interfaces between CuOFHC interlayer and CuCrZr pipe. A maximum size of defect, measured with ultrasonic testing, was defined as a condition of the acceptance of components from the manufacturer. All the 456 PFUs received at CEA were inspected by UT by the manufacturer and are compliant with the acceptance criteria. Reception tests led by CEA (IR, HHF) confirm that most of the delivered PFUs have the required heat load handling capability. 108 PFUs were tested using IR. Eight PFUs (~7%) revealed thermal imperfections on 46 blocks, one PFU concentrating thermal imperfections on all its blocks. The proportion of blocks with defect detected by IR among all the 108x35 blocks is low (1.2%). Among the eight PFUs with detected defects, four of them have imperfections only on the blocks located at PFU's extremity. Those PFUs were installed in WEST as the blocks are located in a zone with negligible heat load. About the four other PFUs, the detected defects are located at different zones and UT did not detect any imperfection on them. To evaluate the possibility of installing these PFUs in WEST, HHF tests are used. The HHF results are fully consistent with the IR results.

1 Introduction

On the road to the fusion energy, ITER will be a great achievement. However, sufficient experience feedbacks, from different fusion devices all around the world, are needed to ensure the success of ITER. CEA contributes to this aim through the WEST tokamak operation. Indeed, WEST lower divertor was upgraded to operate under relevant plasma configurations manufacturing technologies options foreseen for the ITER divertor target. The WEST components, so called Plasma Facing Units (PFUs), were industrially manufactured by AT&M company (China) using hot isostatic pressing (HIP) for bonding tungsten blocks to copper-chromium-zirconium (CuCrZr) pipe with an intermediate pure copper (Cu-OFHC) ring [1]. After the different manufacturing steps, some tests were performed by the manufacturer (dimensional controls and ultrasonic testing (UT)) [2]. One of the detrimental defects, leading to non-adequate heat load handling capability during WEST operation, are defects localized at W to Cu-OFHC and Cu-OFHC to CuCrZr interfaces [3]. Reception tests performed at CEA (infrared (IR) thermography non-destructive testing and high heat flux (HHF) tests performed in collaboration with IPP) lead to confirm that most of the delivered PFUs have the required heat load handling capability [4]. The aim of this study is to present the results of defect detection. For this, cross-checking of all available data (from UT, IR thermography and HHF tests) is performed. Such approach is proposed as those examinations use different techniques to detect the presence of studied defects. The first part of this paper describes the PFU and the techniques used for the

¹ To perform this study, the first author was affiliated to CEA. Now the first author is affiliated to Aix – Marseille Univ., CNRS, Centrale Marseille, LMA, Marseille, France

detection of the studied defects (section 2). The second part presents the IR thermography facility, called SATIR, and the process used to obtain the results from this examination (section 3). The third part relates the SATIR results (section 4). The last part exhibits the UT, IR thermography and HHF tests correlations (section 5).

2 Plasma facing unit and detection of potential thermal imperfection

2.1 PFU description

The actively cooled PFU [5] is designed to withstand high level of heat load: 10MW/m^2 in steady state and 20MW/m^2 in transient [6]. WEST's lower divertor will be composed of 12 sectors, each one consisting of 38 PFUs (Figure 1) [7]. A PFU consists of 35 tungsten (W) blocks (also called monoblocks) - equipped with Cu-OFHC interlayer - mounted on a CuCrZr cooling pipe by HIP[1].

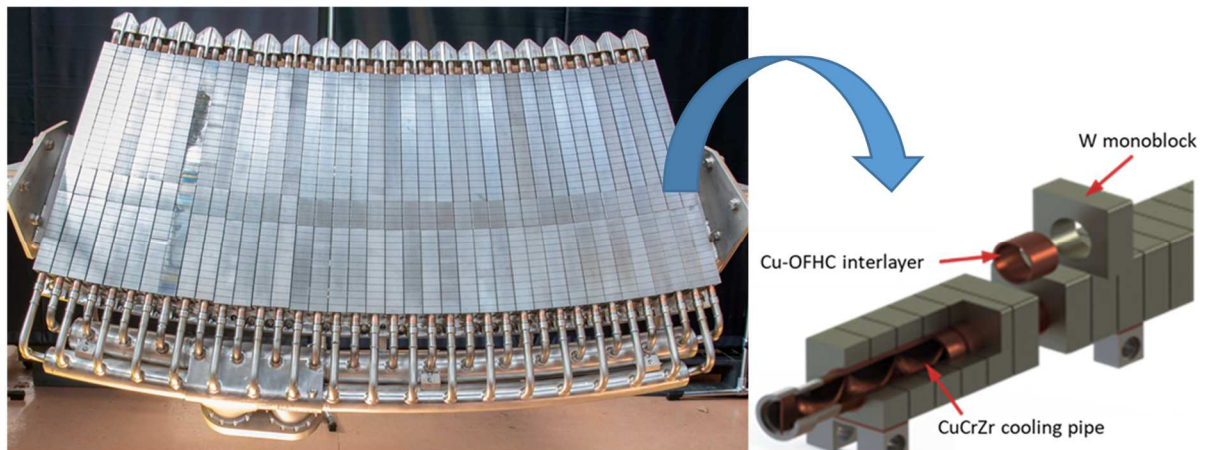


Figure 1 : An overview of a sector composed of 38 PFUs and a detailed illustration of a PFU

2.2 Non-destructive testing

As described in [2], imperfections at interface are quantified by their position ($\theta / ^\circ$), extension ($\Delta\theta / ^\circ$) and axial length ($\Delta X / \text{mm}$) (Figure 2). The maximum acceptable size of defect is set to fulfill acceptance criteria defined for the ITER inner vertical targets. It has to be noted that the WEST PFU acceptance criteria is more restrictive than this reference. This was possible owing to the feedback provided by AT&M company on the achievable quality after manufacturing. To ensure the acceptance of PFUs with acceptable interface quality non destructive tests (NDT) are performed. Ultrasonic testing (UT) is performed by the manufacturer itself. IR thermography and HHF, led by CEA, are performed as acceptance tests. In this section, we will present the UT and the HHF tests while the IR thermography (SATIR facility) will be the subject of the next section.

2.2.1 Ultrasonic testing (UT)

The inspection is performed from the internal pipe's surface [8]. A part of the ultrasound's energy is reflected back to the emitter by the interfaces due to the impedance contrasts between materials, while the other part continues propagating. An abnormal level of signal from an interface indicates a debonding/delamination at this interface (total reflection of the ultrasonic wave). For the inspection of the PFUs, the UT probe parameters are: ultrasonic wave frequency of 15MHz, a focal length of 11mm, a scan speed: lower than 100mm/s and a pulse frequency of 1kHz. With this method ($\Delta\theta=14^\circ$,

$\Delta X=2\text{mm}$) size defect may be detected at CuOFHC to CuCrZr interface while defect size of ($\Delta\theta=8^\circ$, $\Delta X=1\text{mm}$) may be detected at W to CuOFHC interface.

To accept the components after their manufacturing, one of the criteria is to fulfill the following acceptance criteria [2]:

- For $-120^\circ < \theta < 120^\circ$, $\Delta\theta < 45^\circ$.
- For other θ , $\Delta\theta < 50^\circ$.
- $\Delta X < 4\text{mm}$.

All the 456 PFUs received at CEA were inspected by UT and are compliant with the acceptance criteria (see section 5.1).

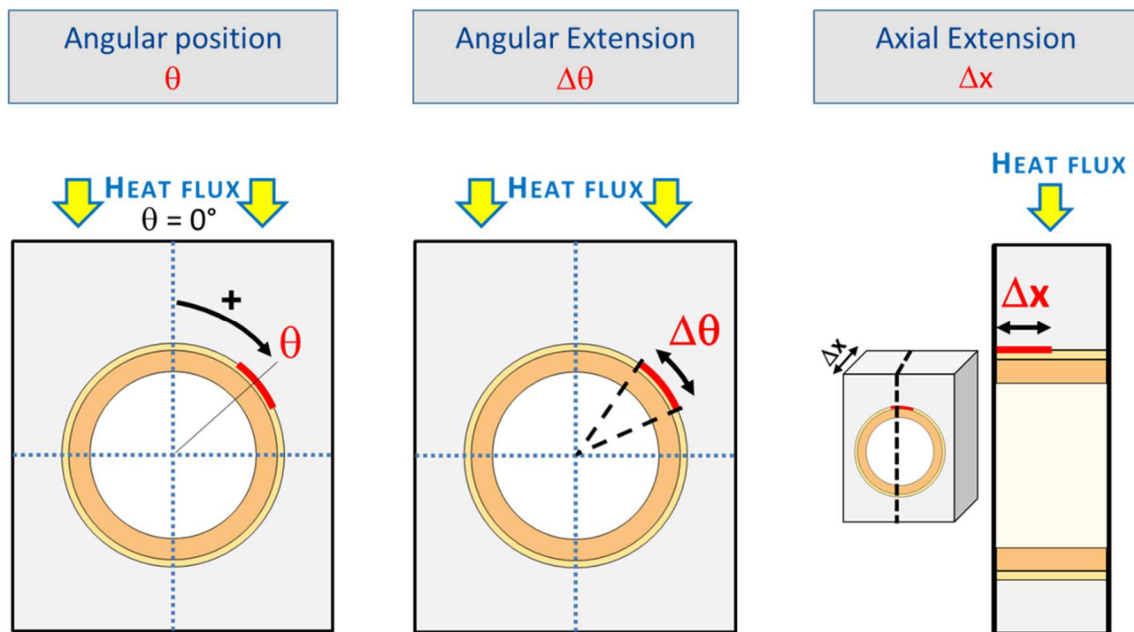


Figure 2: Typical defect's parameters (defect is sketched in red)

2.2.2 High heat flux (HHF) tests

Functional tests as HHF tests are interesting because they allow checking the behavior of the component under representative heat loads. For the PFU, they consist in cycling components in the range of 100 cycles at 10MW/m^2 [4] in steady state for 10s. The surface temperature is monitored during cycling in order to measure a possible evolution. The difference of surface temperatures, estimated at given positions and number of cycles, is defined as assessment criteria [4]. The assessment criteria (ΔT_{100}) is the surface temperature difference between the 100th cycle and the 1st cycle [4]. For the moment, no maximum limit has been set to declare the quality of the component as questionable [2]. In total, 13 PFUs were HHF tested ($\sim 3\%$) [2] within GLADIS facility at IPP [4] and within HADES facility at CEA [2]. For the temperature assessment, emissivity is taken into account. For GLADIS, the method is described in [4]. For HADES testing, emissivity is measured before and after HHF tests on the whole PFU using the method described in [9].

3 SATIR test and related data process developed for the industrial series manufacturing of the WEST PFUs

3.1 General description

IR thermography is performed on the SATIR (Station d'Acquisition et de Traitement InfraRouge) facility at CEA. It has shown a great relevancy for the qualification of actively cooled plasma facing components (PFCs) for Tore Supra and W7-X [10][11]. It has also emphasized an added value, in parallel with UT, as a NDT tool for several mock-ups manufactured and tested through HHF tests for the development of the DEMO divertor target [12]. For the testing of PFUs, a new test set-up and protocol have been used in order to face the testing of an industrial series manufacturing.

This IR NDT technique lays on a straightforward principle: comparing the thermal response of the tested component during a transient thermal load with the thermal response of a “reference” defect-free component. To do this, SATIR shot is organized as follow: hot water (typically $\sim 100^{\circ}\text{C}$) is injected through the cooling pipe of the tested component with specific flow rate and pressure (10 bar) set for conditions corresponding to the circulation of hot water ($4\text{m}^3/\text{h}$) [13]. Then, cold water (typically $\sim 10^{\circ}\text{C}$) is abruptly injected in the cooling tube. An infrared camera [$3\text{--}5\ \mu\text{m}$] records the thermal response of the component's surface facing the camera. A suitable processing is then carried out in order to obtain a temperature movie ($^{\circ}\text{C}$) that is pixel-wise estimated [13]. Emissivity and background temperatures, necessary for the temperature assessment, are taken into account and estimated according to the method presented in [13]. The W emissivity is considered as constant for the camera wavelength range [$3\text{--}5\ \mu\text{m}$] and for the test temperature range [$10\text{--}105^{\circ}\text{C}$].

Such test is particularly suited for actively cooled PFC that have thermal heat exhaust function. Depending on the need, the testing is performed in order to obtain the thermal answers of all the external surfaces of the components.

If until now a physical reference was used as reference [13], a numerical reference has been developed since few years and validated for the first time for the qualification of industrially manufactured PFUs. This choice was motivated by two facts: It is difficult to ensure the complete integrity of a chosen physical reference (a PFU that would be completely free of defect at any time) and two of the three lines would be available for the tests as one is dedicated to the physical reference (Figure 3).

For the purpose of the acceptance tests at CEA, and considering the number of tests to be performed, results from this NDT are assessed from the testing and processing of the plasma facing surface. 108 PFUs among the 456 delivered PFUs were tested on SATIR (24%). Among them, 13 PFUs were tested on SATIR both before and after HHF tests.

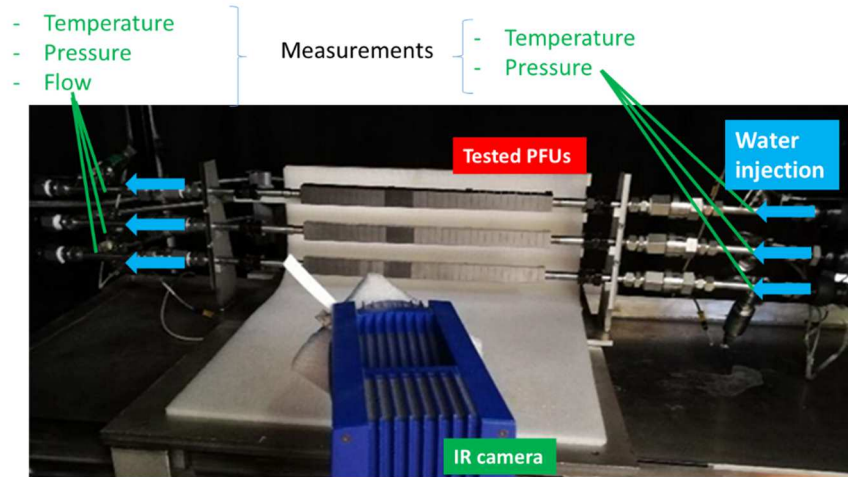


Figure 3: SATIR test set-up (blue : hydraulic lines / green : diagnostics)

3.2 Numerical reference

The numerical reference is a finite element model (FEM) of a PFU (35 blocks modeled) aiming to model the thermal response of all the PFUs which handled SATIR tests. This model is implemented in Ansys V19© software. For each tested PFU, the numerical reference takes as input the measured thermo-hydraulic conditions flowing in the cooling tube during SATIR test. For this, temperature and convective heat transfer coefficient, as function of time, are interpolated from experimental data. This is possible thanks to the thermocouples located at cooling pipe's at the inlet and outlet of each testing line. 2D FEM models are used to model blocks #2 to #34 (width varying to discriminate block from block) while, due to the non-uniform cooling characteristics at the PFU's extremities, 3D FEM models including "a part of the cooling pipe" are indispensable to model accurately the two extreme blocks (#1 and #35) (Figure 4).

The thermal responses of the numerical references (corresponding to the modeling of all the blocks of the first six PFUs tested under HHF tests at GLADIS) were obtained. These PFUs show a good quality during HHF tests (no overheating). For the simulations of the SATIR tests, various combinations of materials properties (thermal conductivity k , specific heat c_p and density ρ) and geometrical dimensions within the specified requirements were carried out. The conclusion is that a shift from the nominal materials properties of all materials ($k + 5\%$ / $c_p - 10\%$) is necessary to obtain a difference of 1 % between the experimental and numerical temperature responses. Nominal materials properties from ITER material handbook are used as in [14].

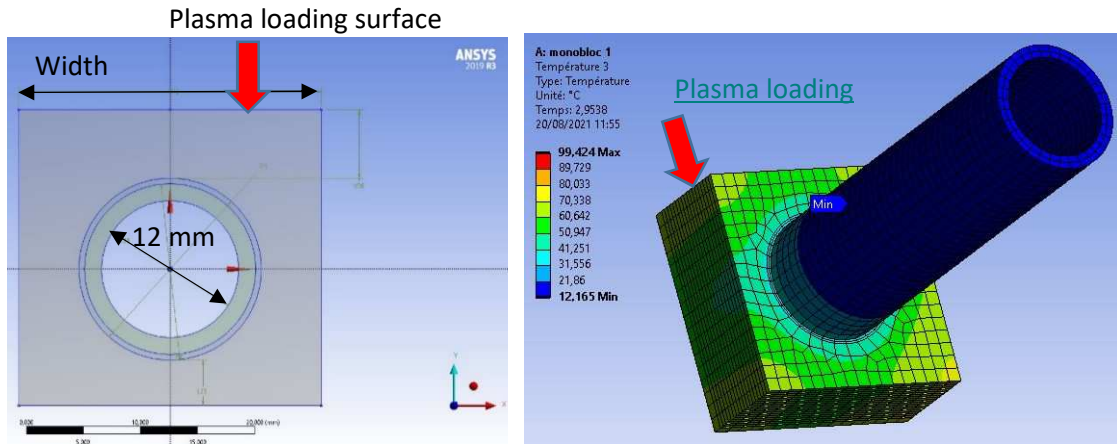


Figure 4: Illustrations of PFU's FEM model : left = 2D with customizable block's width (#2 to #34); right = 3D taking into account a part of the CuCrZr cooling pipe (#1 and #35)

3.3 Acceptance criteria

For each pixel of the numerical and experimental films, the DTRef is calculated. This parameter corresponds to the maximum difference between the experimental (test) and the numerical (reference) temperatures over the transient duration [13]. A DTRef mapping of each W block gives a full visual representation of the component's thermal integrity. Examples of maps are provided in Figure 8. At this step, it is important to be able to distinguish, from these cartographies, a defective zone from acceptable deviations, as a perfect match with the reference is clearly impossible.

Checking all the DTRef maps of more than 3800 W blocks would have cost a tremendous amount of time. Thresholds, applied to the DTRef values, are taken to identify "thermal imperfection" assigned to a defect. A parameter of interest was used for the WEST PFUs reception: the DTRefmax. This is the maximum value of DTRef per block. Based on the relation between DTRefmax and the thermal behavior of the PFUs under HHF test established at CEA during the WEST phase 1 [2], a maximum value of 6°C has been set to state the quality of the component as questionable. Indeed, among all the PFUs tested under HHF test, during HHF tests, no overheating was detected nor inhomogenous distribution was emphasized [2]. For those PFUs, before HHF tests, the maximum DTRefmax is 6°C.

3.4 Measurement uncertainty

To make SATIR test a relevant decision support tool, the deviation assessment of measured DTRefmax is essential. Some experimental factors affect the results issued from the tests (testing conditions, ...). The pragmatic way to define deviation was to carry out an extensive experimental campaign, facing as much as possible the different existing test configurations (testing PFU on the three possible hydraulic lines, mounting and dismounting PFU on the same line). For that, three different PFUs were tested on the three different hydraulic lines (each PFU was positioned once mounted on up, medium and bottom lines) with five shots for each position. In total, for each block 15 shots were used to define the DTRefmax deviation according to (1) :

$$\left| Deviation_{i,n} \right| = \left| \frac{\sum_{i=1}^{15} DTRefmax_i}{15} - DTRefmax_{i,n} \right| \quad (1)$$

where i is the shot number, n is the block number

In total, the results of 15 different SATIR tests obtained on each of the 105 blocks (3 PFUs, 35 blocks per PFU) are treated to perform the repeatability test. The maximum deviation is 2.7°C (Figure 5). This is quite high but it is important to notice that 95% of the estimated deviations are under 1.5°C.

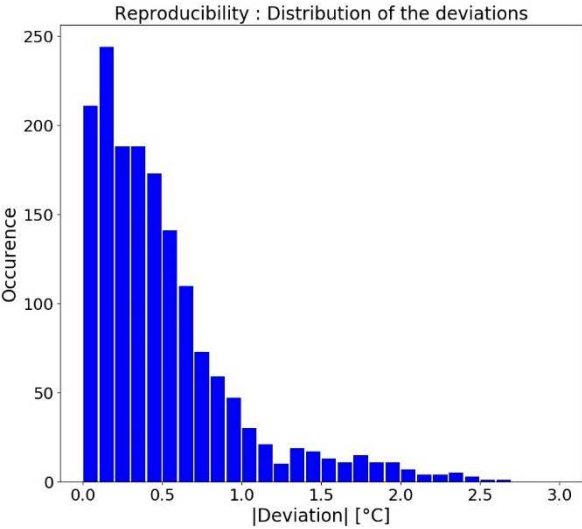


Figure 5: Distribution of the DTRefmax deviations (15 shots x 35 blocks x 3 PFUs)

4 SATIR results

The majority of the PFUs tested with SATIR were randomly chosen from the production. Some of the tested PFUs have acceptable imperfections detected by UT (Figure 6). The DTRefmax distribution is plotted in Figure 7 (up). The DTRefmax distribution corresponding to DTRefmax complying with specifications (<6°C) is presented (Figure 7, down). One can note that no occurrence is presents at 0°C. This may be explained by the fact that DTRefmax is the maximum value of the temperature difference between the reference and the tested PFU, there is consequently a very low probability that the reference perfectly matches the tested PFU. The distribution is centered at 1.03°C and presents a standard deviation of 1.2°C. A determination coefficient of R² of 0.8 is obtained with Gaussian fitting curve. The relatively good fit (R²) of the DTRefmax distribution to the Gaussian distribution highlights a satisfactory quality of the industrial manufacturing process to produce PFUs with some confidence to fulfil the specifications regarding the DTRefmax [2].

Among the 3780 tested blocks (108 PFUs x 35 blocks), 46 blocks have a questionable thermal response as their DTRefmax are higher than 6°C. 8 PFUs (PFU#010, #082, #132, #268, #266,#551, #022, #300) are concerned, one of them (PFU#300) concentrating 35 of the 46 identified blocks. Figure 8 shows the DTRef maps of the blocks with thermal imperfections. The probability to obtain one PFU with defect is 7%. The proportion of blocks with defect detected by IR among all the 108x35 blocks is very low (1.2%).

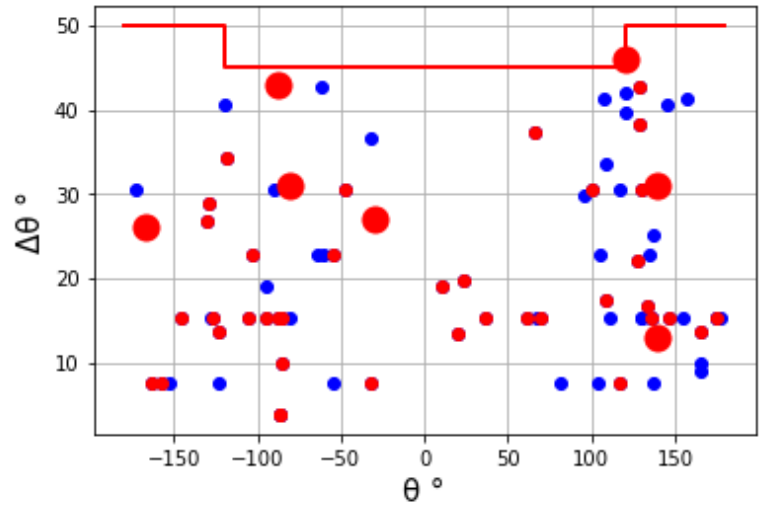


Figure 6 : Acceptable imperfections detected by UT

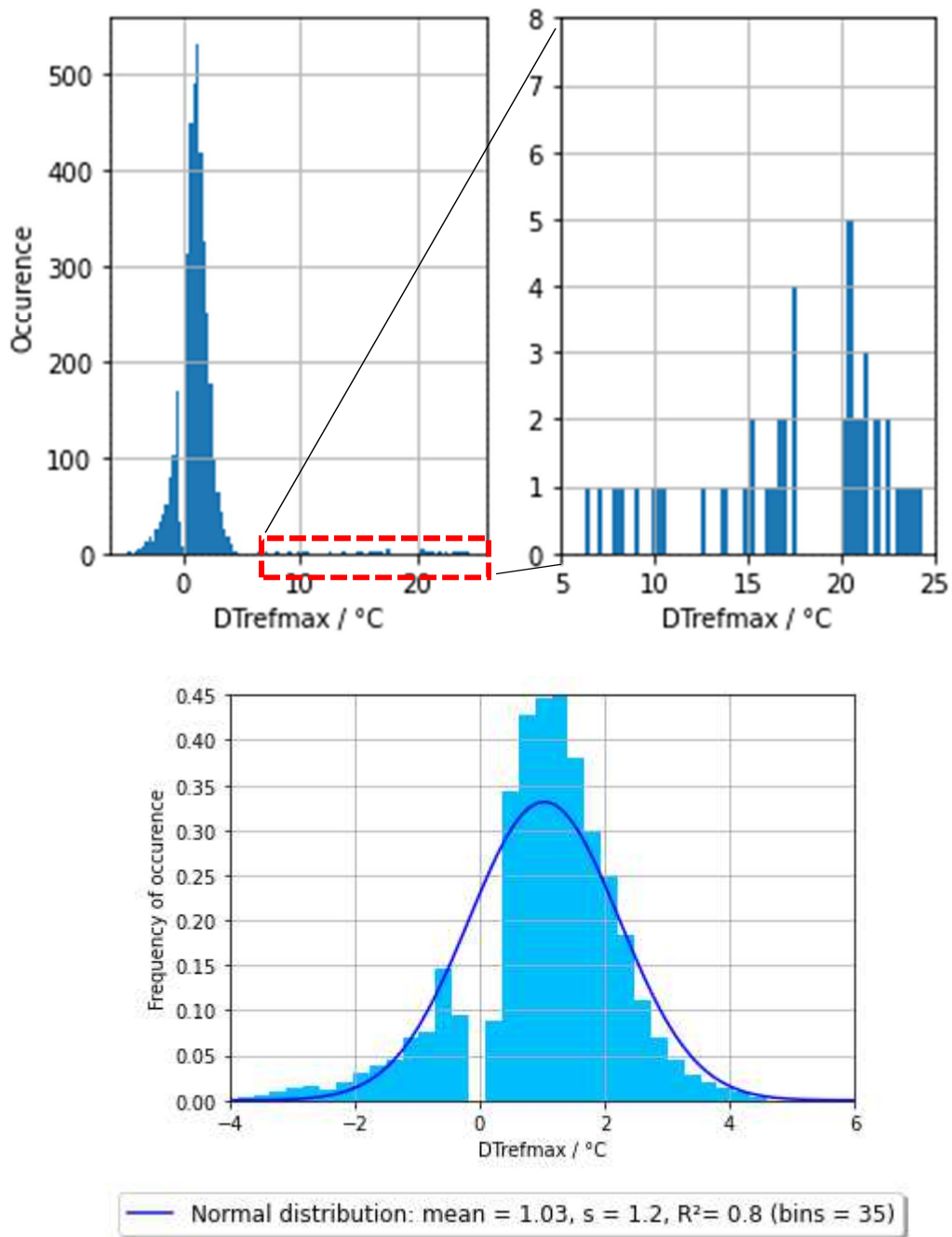


Figure 7: (up) Distribution (bins=100) of all the DTrefmax and insert of the DTrefmax distribution not complying with specifications ($DTREFmax > 6^{\circ}C$) (down) Distribution (bins=35) of DTrefmax complying with specification and related Gaussian fitting curve

(a)

PFU	010	082	132	268	266	551		022			
Block	M1	M35	M35	M34	M13	M3	M8	M32	M33	M34	M35
DTRefmax	8.3°C	9.4°C	6.5°C	7.9°C	7.2°C	12.6°C	10.1°C	10.2°C	13.7°C	15.2°C	10.4°C
DTRef map											
Detected by UT?	NO	YES	YES	NO	NO	NO	NO	NO	NO	NO	NO

(b)

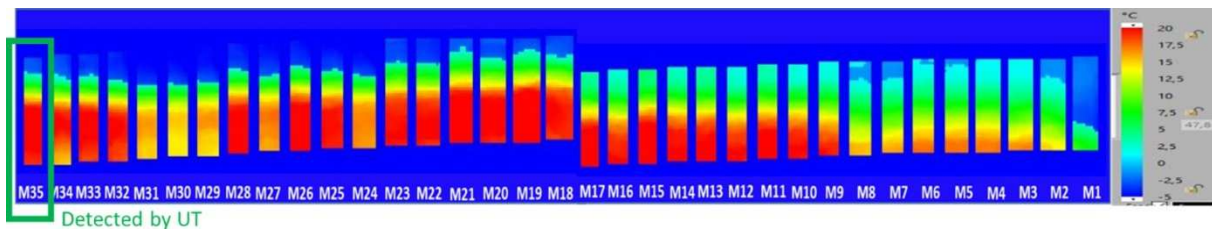


Figure 8 : Blocks/PFUs with thermal imperfections detected with SATIR tests (plasma facing surface view) (a) PFUs#010, #082, #132, #268, #266, #551, #022 (b) DTRef map of the 35 blocks of the PFU#300 (plasma facing surface view)

5 Cross-correlation of UT/HHF/SATIR results to provide PFUs acceptance decisions

5.1 Cross-correlation of UT and SATIR results

According to UT, among the 456 PFUs delivered to CEA, 83 acceptable imperfections are present within 64 different PFUs (14% of the delivered PFUs) (Figure 6). The blocks examined with SATIR and HHF tests are also displayed on this figure. Imperfections are mainly located on the first (30%) and the last blocks (60%). Such defects may be linked to the HIP manufacturing process.

Among the 3780 tested blocks on SATIR, 46 blocks (concerning 42 PFUs) were identified by UT with acceptable imperfections (red dots in Figure 6). For the blocks with acceptable imperfections detected by UT and tested on SATIR, three thermal imperfections are detected with SATIR (Figure 9). As thermal imperfection size range is broad (Figure 9), no clear correlation between the imperfections detected by UT and SATIR is emphasized however it is fully consistent with the detection size threshold emphasized in [4].

Among the 46 thermal imperfection emphasized by SATIR (Figure 8a), only 2 are detected by UT. Further investigations are needed (HHF tests, metallographic examinations) to attribute the cause of the thermal imperfections.

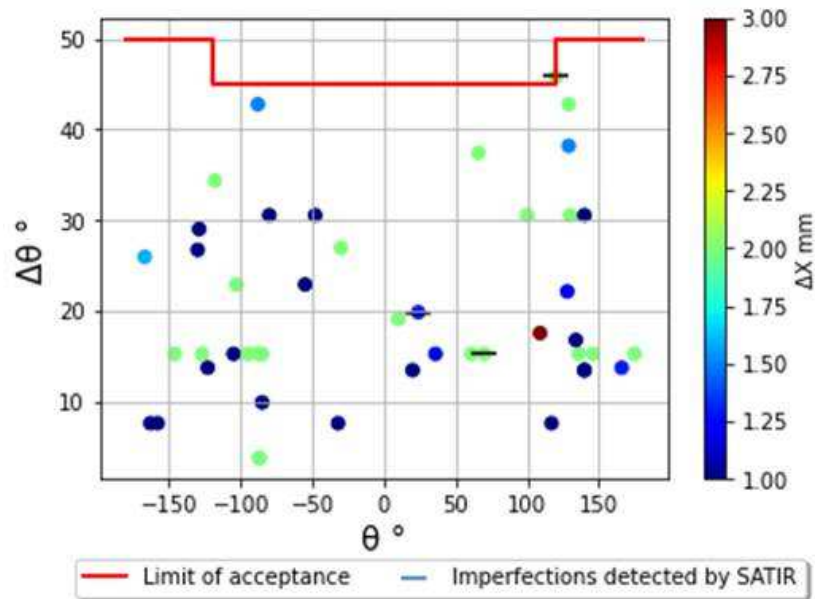


Figure 9 : Imperfections detected by UT and examined on SATIR – Representation of $\Delta X / \text{mm}$ - Three Imperfections are detected both by UT and SATIR

5.2 Cross-correlation of HHF and SATIR results

The results of the HHF testing campaign are reported in [2][4]. For all the HHF tests, no overheating is noticed except for the PFU#300. Due to the high number of defective blocks, PFU#300 was tested on HADES facility and loaded at the particular loading of $6\text{MW}/\text{m}^2$. A surface temperature $\sim 50\%$ higher than the one expected for a PFU without defect was noticed. Those results allow again highlighting the good industrial manufacturing process of the PFUs and the good correlation between SATIR and HHF results.

For the PFUs tested under HHF tests, the comparison between the DTR_{refmax} before and after HHF tests was performed. For all the PFUs, except the PFU#300, no major evolution of the DTR_{refmax} is noticed. All the variations lay within the uncertainty range of $\pm 2.7^\circ\text{C}$ of SATIR tests (section 3.4). The level of solicitation - representative of WEST heat load - could thus be considered as harmless for the component integrity.

5.3 Acceptance decisions for PFUs with thermal imperfections

The blocks located at the PFU extremities of the PFUs are exposed to a very low heat load in WEST [12]. Fortunately, the majority of the blocks with thermal imperfections (Figure 8 up) correspond to zones loaded under reduced heat flux, so that it was decided to derogate the corresponding PFUs (#10, #82, #132, #268) and to mount them onto the WEST lower divertor. As all the blocks of PFU#300 are defective, this PFU is rejected. For the other PFUs of the Figure 8 (#266, #551 and #022), no decision has been yet stated since HHF tests has to be performed to take a final decision about their acceptance. This will be also the opportunity to address a correlation between the NDT techniques data and to better understand any defects growing mechanism due to thermal loads.

In total, 346 PFUs were installed in WEST without being tested with infrared thermography. The results of section 4 enable to conclude that, within the installed PFUs, 24 PFUs (7%) may have thermal imperfections. For these PFUs, thermal imperfection may be present on 145 blocks (1.2%).

Majority of the detected thermal imperfections are localized on the blocks at PFU extremities, consequently the risk was taken to install PFUs without systematic HHF tests. However, to reduce the risk, thermal answer of the PFUs installed in WEST will be monitored with the WEST infrared camera monitoring system.

6 Conclusion

108 PFUs were tested by infrared thermography on SATIR during the reception phase of the WEST PFUs, corresponding to up to 3800 blocks, all of them were tested by UT. Among them: 46 blocks with “acceptable” defects were detected by ultrasonic testing and 46 blocks with thermal imperfections were detected by SATIR. 3 thermal imperfections are detected with the two techniques. This mismatch can be explained partially by the fact that those thermal imperfections are below the acceptance limit in terms of defect size. The NDT techniques highlight the good manufacturing quality (1.2% of blocks present potential thermal imperfections, and stability of the production for blocks without potential thermal imperfection), confirmed by the HHF tests performed on sampled PFUs.

The fact that UT didn’t detect thermal imperfections on 8 PFUs, especially the PFU#300 having 35 “defective” blocks confirmed by high heat flux testing, is not explained yet. Metallographic analysis of the PFU#300 is planned. Finally, this study leads to highlight the complementarity of ultrasonic testing and thermally based NDT (IR thermography). It also pointed out the importance of data cross-correlation between all the techniques (UT, IR, HHF) in order to consolidate relevant diagnosis during a reception phase.

7 Acknowledgments

This work has been carried out within the framework of the EUROfusion Consortium and has received funding from the Euratom research and training programme 2014-2018 and 2019-2020 under grant agreement No 633053. The views and opinions expressed herein do not necessarily reflect those of the European Commission.

8 Bibliography

- [1] M. Firdaouss *et al.*, “First feedback during series fabrication of ITER like divertor tungsten components for the WEST tokamak,” *Phys. Scr.*, 2021, doi: 10.1088/1402-4896/ac2978.
- [2] M. Richou *et al.*, “Acceptance tests of the industrial series manufacturing of WEST ITER-like tungsten actively cooled divertor,” *Phys. Scr.*, vol. 96, no. 12, 2021, doi: 10.1088/1402-4896/ac2657.
- [3] F. Escourbiac *et al.*, “Experimental activity on the definition of acceptance criteria for the ITER divertor plasma facing components,” *Fusion Eng. Des.*, vol. 84, no. 2–6, 2009, doi: 10.1016/j.fusengdes.2009.01.072.
- [4] H. Greuner, B. Böswirth, M. Lipa, M. Missirlian, and M. Richou, “Results of high heat flux qualification tests of W monoblock components for WEST,” in *Physica Scripta*, 2017, vol. 2017,

- no. T170, doi: 10.1088/0031-8949/2017/T170/014001.
- [5] M. Missirlian *et al.*, "The WEST project: Current status of the ITER-like tungsten divertor," *Fusion Eng. Des.*, vol. 89, no. 7–8, 2014, doi: 10.1016/j.fusengdes.2014.01.050.
 - [6] T. Hirai *et al.*, "ITER divertor materials and manufacturing challenges," *Fusion Eng. Des.*, vol. 125, pp. 250–255, 2017, doi: 10.1016/j.fusengdes.2017.07.009.
 - [7] J. Bucalossi *et al.*, "The WEST project: Testing ITER divertor high heat flux component technology in a steady state tokamak environment," *Fusion Eng. Des.*, vol. 89, no. 7–8, 2014, doi: 10.1016/j.fusengdes.2014.01.062.
 - [8] G.-N. Luo *et al.*, "Overview of decade-long development of plasma-facing components at ASIPP," *Nucl. Fusion*, vol. 57, no. 6, 2017, doi: 10.1088/1741-4326/aa6502.
 - [9] J. Gaspar *et al.*, "Emissivity measurement of tungsten plasma facing components of the WEST tokamak," *Fusion Eng. Des.*, vol. 149, 2019, doi: 10.1016/j.fusengdes.2019.111328.
 - [10] M. Missirlian *et al.*, "Qualification of high heat flux components: Application to target elements of W7-X divertor," *Phys. Scr. T*, vol. T128, pp. 182–188, 2007, doi: 10.1088/0031-8949/2007/T128/035.
 - [11] A. Durocher *et al.*, "Advanced qualification methodology for actively cooled plasma facing components," *Nucl. Fusion*, vol. 47, no. 12, pp. 1682–1689, 2007, doi: 10.1088/0029-5515/47/12/006.
 - [12] F. Gallay *et al.*, "Quantitative thermal imperfection definition using non-destructive infrared thermography on an advanced DEMO divertor concept," in *Physica Scripta*, 2017, vol. 2017, no. T170, doi: 10.1088/1402-4896/aa878e.
 - [13] N. Vignal *et al.*, "Improvement of non destructive infrared test bed SATIR for examination of actively cooled tungsten armour Plasma Facing Components," *Fusion Eng. Des.*, vol. 88, no. 9–10, 2013, doi: 10.1016/j.fusengdes.2013.05.053.
 - [14] M. Richou *et al.*, "Fatigue lifetime of repaired high heat flux components for ITER divertor," *Fusion Eng. Des.*, vol. 86, no. 9–11, 2011, doi: 10.1016/j.fusengdes.2011.03.020.